J Porous Mater (2015) 22:339–345
DOI 10.1007/s10934-014-9901-9

Application of mesoporous ZSM-5 as a support for Fischer–Tropsch cobalt catalysts

Yuelun Wang · Weiming Zhao · Zhuo Li · Hui Wang · Jinhu Wu · Min Li · Zhiping Hu · Yongshen Wang · Jun Huang · Yunpeng Zhao

Published online: 23 December 2014

Abstract The effect of mesoporous structure of ZSM-5 on the properties of cobalt-based catalysts for Fischer–Tropsch synthesis was studied in this work. ZSM-5 and amorphous SiO_2 supports have also been applied for comparison. It was shown that post treatment of ZSM-5 catalyst by NaOH solution improved the catalytic performance to produce higher amount of liquid hydrocarbons. The hierarchical structure combining with the acidity of meso-ZSM-5 had great effect on increasing the selectivity to $C_{5–18}$ hydrocarbons and preventing the formation of CH_4. The more acid sites of the support promoted catalytic cracking reaction of olefinic hydrocarbons to light hydrocarbons, the lower olefin to paraffin ratio was observed over Co/meso-ZSM-5 catalyst compared with that of Co/SiO_2 catalyst.

Keywords Fischer–Tropsch synthesis · NaOH treatment · Mesoporous ZSM-5 · Cobalt catalyst

Y. Wang · W. Zhao · M. Li · Z. Hu · Y. Wang · J. Huang · Y. Zhao
Key Laboratory of Coal Processing and Efficient Utilization, Ministry of Education, China University of Mining and Technology, Xuzhou 221116, Jiangsu, China

Y. Wang (✉)
School of Chemical Engineering, China University of Mining and Technology, Xuzhou 221116, Jiangsu, China
e-mail: wangyuelun@126.com

Z. Li · H. Wang · J. Wu
Key Laboratory of Biofuel, Chinese Academy of Sciences, Qingdao Institute of Bioenergy and Bioprocess Technology, Qingdao 266101, China

1 Introduction

Fischer–Tropsch (FT) synthesis for the conversion of synthesis gas to hydrocarbons has attracted great interests as an important process for the production of transportation fuels and chemicals [1]. It offers the possibility of converting a mixture of hydrogen and carbon monoxide into clean hydrocarbons, free from sulfur [1, 2]. Over conventional FT catalysts, hydrocarbon products generally follow the Anderson-Schulz-Flory (ASF) distribution, which is wide and unselective to products ranging from CH_4 to heavy waxes [3]. The development of novel catalysts that can tune product selectivity would significantly improve the FT technology. Cobalt based catalysts are widely applied for FT synthesis because of their high activity, low water–gas shift activity, high selectivity to long chain hydrocarbons and low operating temperature [4, 5].

There are many factors that influence catalytic selectivity including used support materials, support pore size, metal particle size, and promoters, in addition to the operating parameters such as temperature, pressure, and feed composition, etc. Especially, the physicochemical properties of supports have a great effect on the size, dispersion and catalytic performance of cobalt catalysts [6, 7]. Many researchers are interested in the production gasoline fraction in FT synthesis using ZSM-5 [8, 9] as the support. Besides this zeolite, mordenite [10], MCM-22 [11], β [12] and ITQ [13] etc. have also been used. However, the pores of zeolites consist of micropores which are not large enough to transfer larger molecules. The slow transportation of products inside the long micropores of zeolites usually causes over-cracking, leading to high selectivity to undesirable light hydrocarbons (CH_4 and $C_{2–4}$ alkanes). To solve this problem, the support with two kinds of adjustable pore diameters (bimodal porous materials) is required. The

introduction of mesopores into zeolite crystals was tried. Such structure may give rise to the possibility to increase branched products with the higher octane number because the large space of the mesoporous material around an active acid site in zeolite promotes the generation of the more bulky branched hydrocarbons and decreases the selectivity of methane. Yang et al. [14] prepared a novel zeolite capsule catalyst with a specific core (Co/SiO_2)-shell structure. The capsule catalysts exhibited higher selectivity of isoparaffins than that of the naked Co/SiO_2 catalyst in FT synthesis due to the space confined effect. Kang et al. [15] investigated the effects of ZSM-5 modification on the Co/SiO_2 catalyst and the maximization of C_{5-22} hydrocarbon selectivity was obtained by varying the content of ZSM-5. They attributed to the formation of a small crystallite size of cobalt oxide and the optimum acid site density on ZSM-5 by the possible migration of cobalt crystallites from Co/SiO_2 to the ZSM-5 surface. Kang et al. [16] found that mesoporous ZSM-5 supported Ru catalyst prepared by a simple NaOH treatment of H-ZSM-5 could significantly improve the product selectivity of C_{5-11} isoparaffins. Sartipi et al. [17] used mesopores H-ZSM-5 supported cobalt as a bifunctional catalyst in FT synthesis resulting in a high selectivity to liquid fractions. Meanwhile, high methane selectivity was obtained due to strong Co-zeolite interaction leading in formation of more Co particles with low coordination sites.

In order to further study the influence of mesoporous structure of zeolite on tuning the product selectivity over cobalt-based catalysts in FT synthesis, Co/meso-ZSM-5 catalyst compared to Co/ZSM-5 and conventional Co/SiO_2 catalyst was discussed in this article.

2 Materials and methods

2.1 Samples preparation

ZSM-5 was prepared as follows: first, 2.409 g of sodium aluminate was dissolved in 37.8 mL of tetrapropylammonium hydroxide (25 %), together with 65.5 mL of water and 0.191 g of sodium hydroxide, a certain amount of TEOS were added to this solution. After homogenization, the mixture was heated at 140 °C and kept at this temperature for 72 h. The obtained solid by centrifugation was washed with deionized water and then dried at 60 °C for 12 h. The sample was then calcined at 550 °C for 5 h. Ion exchange was performed using 1 M solution of NH_4NO_3 at 80 °C for 4 h by two consecutive similar processes. After the ion exchange, the zeolite was filtered and washed with enough de-ionized water and after that dried in oven at 90 °C overnight, the NH_4-ZSM-5 was calcined in the static air at 500 °C for 3 h to obtain H-ZSM-5.

Meso-ZSM-5 was prepared using a simple alkaline treatment method. Briefly, the experiment was carried out in a 250 cm^3 round-baker adapted to a reflux-condenser filled with aqueous 0.5 M NaOH at 70 °C for 30 min. After treatment, the solid zeolite was recovered by filtration, washing with deionized water, drying, and calcination in air at 300 °C for 5 h.

The supported cobalt catalysts were prepared by initial wetness impregnation method. For comparison, conventional ZSM-5 zeolite supported cobalt catalyst and conventional SiO_2 supported cobalt catalyst were also synthesized, respectively. 3 g of different supports were completely wetted with deionized water to evaluate the corresponding volume. Then, cobalt nitrate was dissolved into the required deionized water to impregnate the supports with the loading of 15 %. The catalysts were then dried under temperature of 60 °C and calcined at 400 °C for 4 h. The obtained catalysts were named Co/meso-ZSM-5 catalyst, Co/ZSM-5catalyst and Co/SiO_2 catalyst, respectively.

2.2 Characterization

The textural properties of supports and catalysts were determined by nitrogen adsorption, carried out at −196 °C, in a Micromeritics equipment, model ASAP 2020. Before the analysis, around 0.15 g of the sample was heated at 120 °C for approximately 12 h and then heated up to 200 °C at a rate of 10 °C min^{-1}, maintaining the solid at this temperature for 2 h, under vacuum. The pore size distribution in the mesoporous region was determined by the Barrett–Joyner–Halenda (BJH) method, and that in the microporous region was evaluated by the Horvath–Kawazoe (HK) method. The microporous volume was estimated by the t-plot method.

X-ray diffraction (XRD) patterns of the samples were recorded on a Bruker B5005 diffractometer using Cu K α radiation. The mean Co_3O_4 crystallite sizes were deduced from the XRD data using the Scherrer equation.

TPR was carried out in a U-tube quartz reactor at the ramp rate of 10 °C min^{-1} in the 5 % H_2/Ar (vol.) flow of 30 mL min^{-1}. The H_2 consumption was monitored with TCD using the reduction of CuO as the standard. The reduction percentage of the cobalt oxides at temperatures less than 400 °C was calculated from the TPR profiles.

Scanning electron microscopy (SEM) was performed on a PhilipsXL 20 microscope. Samples were coated with a layer of gold using an Edwards S150A sputter coater, to make them conductive prior to imaging.

Temperature-programmed desorption of ammonia was performed with a Chem TPR/TPD instrument (Quantachrome). Approximately 100 mg catalyst was activated for 1 h at 500 °C heating with a ramp of 10 °C min^{-1}. After

cooling to 200 °C, pure ammonia was passed through the sample. The desorption of the ammonia was accomplished by purging helium with a flow of 20 mL min^{-1} and raising the temperature to 800 °C. The effluent gas was analyzed by an on-line gas chromatograph with a TCD detector.

Catalysts were evaluated in a pressured fixed-bed reactor at 2 MPa, 1,000 h^{-1} with the H_2/CO ratio of two after reduction at 400 °C for 10 h. Wax was collected with a hot trap and the liquid products were collected in a cold trap after 24 h on-stream. The gas effluents were analyzed on-line by using Carbosieve-packed column with TCD. The gas hydrocarbons were analyzed on-line using Porapack-Q column with FID. Oil and wax were analyzed offline in OV-101 capillary columns. 5 % N_2 was added to syngas as an internal standard. The carbon balance and mass balance were 100 ± 5 %.

3 Results and discussion

3.1 Physic-chemical properties of catalysts

Nitrogen physisorption at −196 °C was used to evaluate the textural structure of corresponding catalysts. Figure 1 shows N_2 adsorption/desorption isotherm and pore size distribution of catalysts. The hysteresis loops which were the characteristic feature of type IV isotherm appeared. The isotherms showed the capillary condensation in mesopores and limitation in uptake over the relative high P/P^0. The pore size distribution of the hierarchical ZSM-5 supported cobalt catalyst showed micropores and mesopores (Fig. 1a), respectively. The BET specific surface area of the hierarchical ZSM-5 supported catalyst was 389 m^2 g^{-1}. And its total pore volume increased from 0.26 to 0.60 cm^3 g^{-1} compared to that of ZSM-5. This increase was due to creation of mesopores at the cost of a slight decrease in the zeolite micropore volume. The decrease in micropore volume suggested some minor amorphization during the base treatment due to the desilication [18]. The pore size distribution of ZSM-5 supported catalyst is shown in Fig. 1b, which mainly centered at 1.0 nm. The isotherm showed textural mesopores resulting from the interparticle voids [19]. The BET specific surface area of ZSM-5 supported catalyst is 357 m^2 g^{-1} lower than that of alkaline treated support. As for conventional SiO_2 supported catalyst, wider pore size distribution and higher volume were observed compared to ZSM-5 supported catalyst in Fig. 1c.

XRD patterns of the catalysts are presented in Fig. 2, all catalysts showed the characteristic reflection peak at $2\theta = 36.8°$ due to the presence of Co_3O_4 phase. The crystallite size of Co_3O_4 was calculated by using the Scherrer equation. Cobalt crystallite sizes of 8.2, 11.2, and 16.8 nm were obtained for Co/ZSM-5, Co/Meso-ZSM-5 and Co/SiO_2, respectively, as summarized in Table 1. Clearly, cobalt crystallite size on Co/Meso-ZSM-5 catalysts is larger than that of Co/ZSM-5 catalyst and smaller than that of Co/SiO_2 catalyst. This could be attributed to the pore size distribution of supports. Small pore size distribution was contributed to the small cobalt nanoparticles. The diameter of particles was larger than pore sizes of the support indicating that some Co_3O_4 particles could be located on the external surface of the support. On the other hand, the characteristic peaks of ZSM-5 were clearly observed on Co/ZSM-5 and Co/Meso-ZSM-5 catalysts, suggesting the sustainment of MFI structures on catalysts.

H_2-TPR profiles of all the Co catalysts are plotted in Fig. 3. The Co based catalysts underwent two typical steps during the reduction in the flow of H_2, i.e. Co_3O_4 to CoO and then CoO to Co. The small peak intensity at higher temperature region above 450 °C suggested the interaction between cobalt oxide and the support. Contribution of the high-temperature peaks was more pronounced in the case of Co/ZSM-5 probably due to smaller Co crystallite size, indicating the stronger cobalt-support interaction resulting in lower reduction. Co/meso-ZSM-5 catalyst appearing at around 300 and 337 °C could be assigned to the easily reducible cobalt crystallites to metallic state at lower temperatures. In addition, weak cobalt-support interaction was also presented due to minimal reduction peak observed at high temperature. In the case of Co/SiO_2 catalyst, a reduction profile assigned to Co_3O_4 was observed at temperature region between 290 and 348 °C. Nevertheless, no notable reduction peak of cobalt-support interaction was observed at high temperature. The reduction degree was relatively expressed as the ratio of the amount of H_2 consumption below 400 °C to that of total H_2 consumption. The values were 68.4, 78.6 and 80.4 % for Co/ZSM-5 catalyst, Co/meso-ZSM-5 catalyst and Co/SiO_2 catalyst, respectively, as shown in Table 1.

The SEM micrographs of the samples are shown in Fig. 4. For Co/ZSM-5 catalyst, we can find that the zeolite crystals, with the crystal size of 2–4 μm, were homogeneous and uniform. The images of Co/meso-ZSM-5 catalyst revealed that apart from agglomeration of the zeolite crystallites, their individual size and morphology did not change greatly after alkali treatment. As for Co/SiO_2 catalyst, some smaller particles and larger agglomerated particles with different morphologies were observed, which could be related to agglomeration of cobalt oxide particles in the sample.

The NH_3-TPD patterns of Co/meso-ZSM-5 catalyst and Co/ZSM-5 catalyst are shown in Fig. 5. Two NH_3 desorption peaks were observed. The lower-temperature peak centered at 100–220 °C could be assigned to ammonia desorption over the weak acid sites [18]. It can be observed that the intensity of weak acid sites was higher on

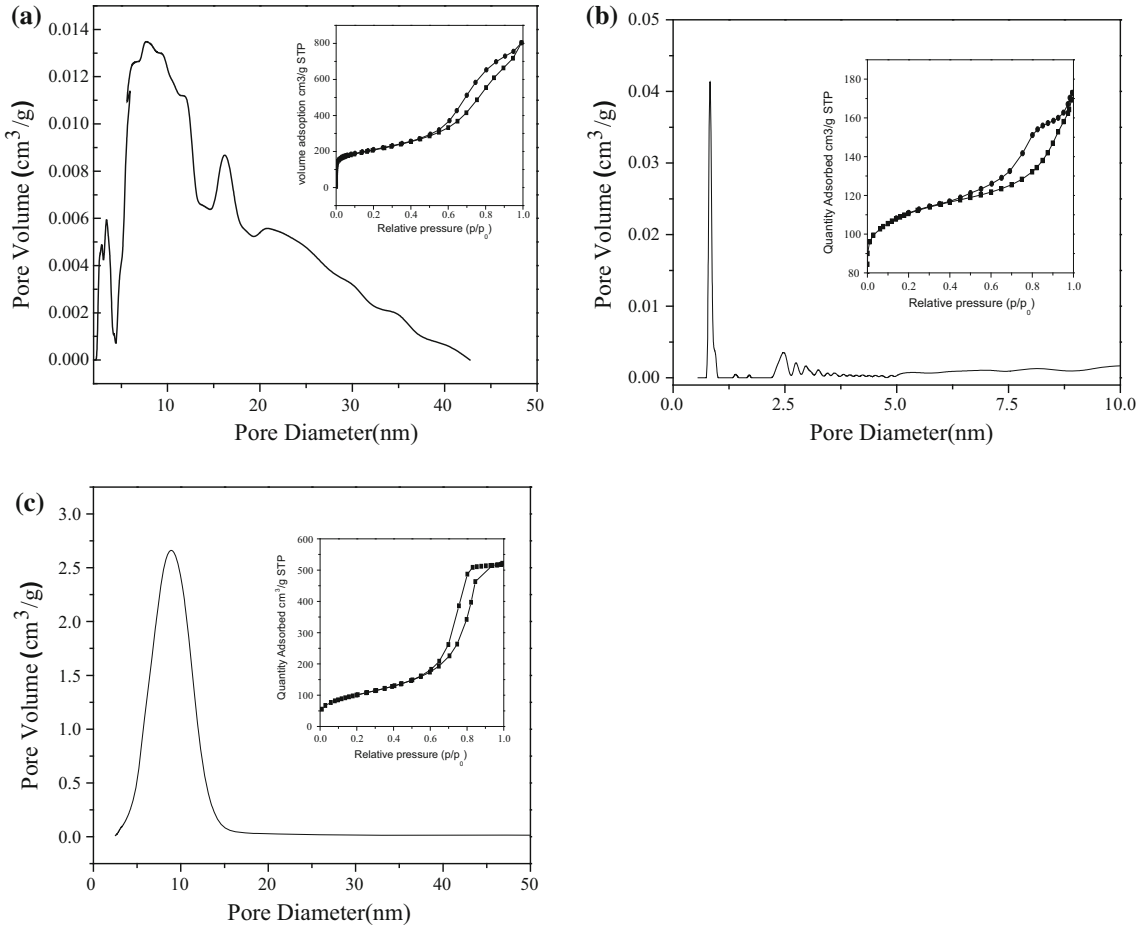

Fig. 1 N_2 adsorption/desorption isotherm and pore size distribution of catalyst. **a** Co/Meso-ZSM-5, **b** Co/ZSM-5, **c** Co/SiO_2

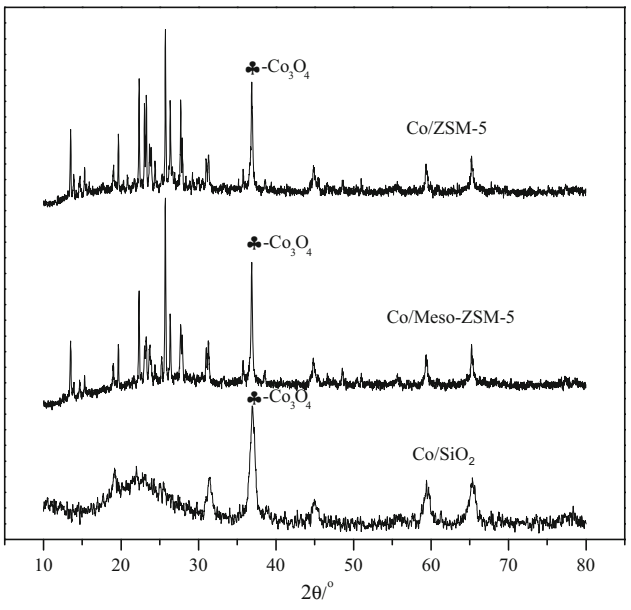

Fig. 2 XRD profiles of the prepared catalysts

Co/meso-ZSM-5 catalyst in the first desorption temperature region. A broad peak at 300–727 °C, which could be attributed to the adsorption of strong acid sites, was observed. Table 1 gives the number of acid sites expressed as mmol NH_3 g^{-1} of catalyst with respect to weak and strong acidic sites. By considering first peak only (weak acid sites), the total number of acid sites increases with the decrease in Si/Al ratio of the support due to the desilication of ZSM-5. Si/Al ratios determined with ICP-OES in ZSM-5 and Meso-ZSM-5 were 78.8 and 68.4, respectively.

3.2 Catalyst evaluation

CO conversion at steady-state was presented in Table 2. The highest conversion was obtained with Co/SiO_2 catalyst due to its highest reducibility as shown by TPR. While ZSM-5 supported Co catalyst showed reduced FT activity as compared with that of Co/SiO_2 catalyst. By introducing porous hierarchy in the zeolite crystallites, the sizes of Co particles increased with the presence of mesoporosity,

Table 1 The structure properties of cobalt catalysts

Samples	Specific surface area ($m^2\ g^{-1}$)	Average support size (nm)	V_{micro} ($cm^3\ g^{-1}$)	V_{meso} ($cm^3\ g^{-1}$)	Average Co_3O_4 particle size (nm)	Reducibility (%)	Total acid sites (mmol $NH_3\ g^{-1}$)
Co/ZSM-5	356.8	2.8	0.17	0.09	8.2	68.4	0.49
Co/Meso-ZSM-5	388.5	6.2	0.22	0.38	11.2	78.6	0.64
Co/SiO_2	346.2	8.5	0.30	0.52	16.8	80.4	–

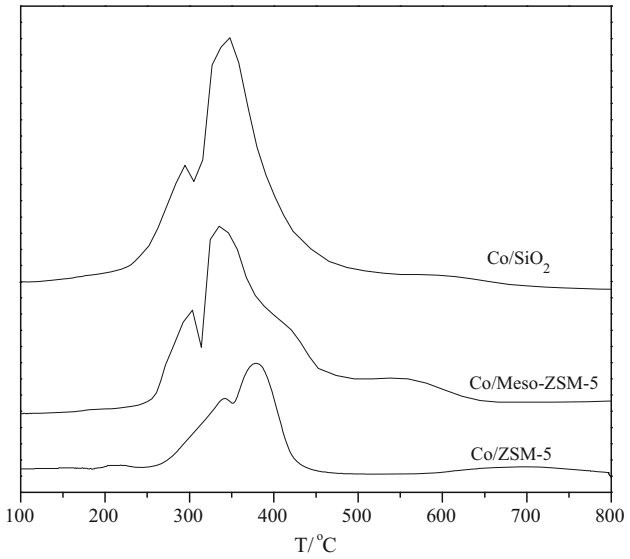

Fig. 3 TPR profiles of the prepared catalysts

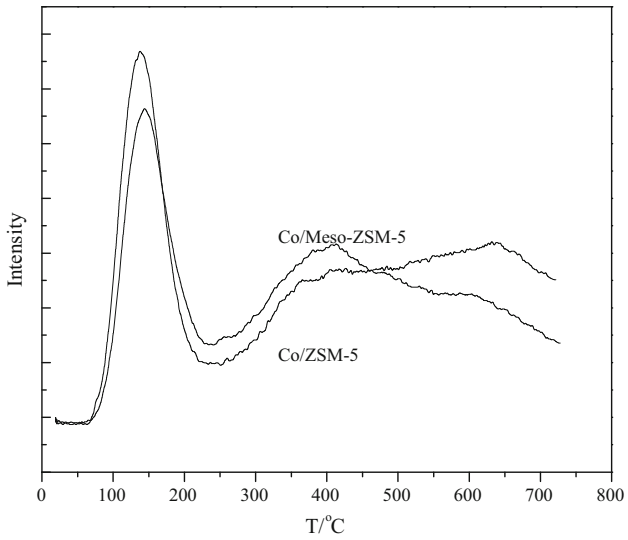

Fig. 5 NH_3-TPD profiles of the prepared catalysts

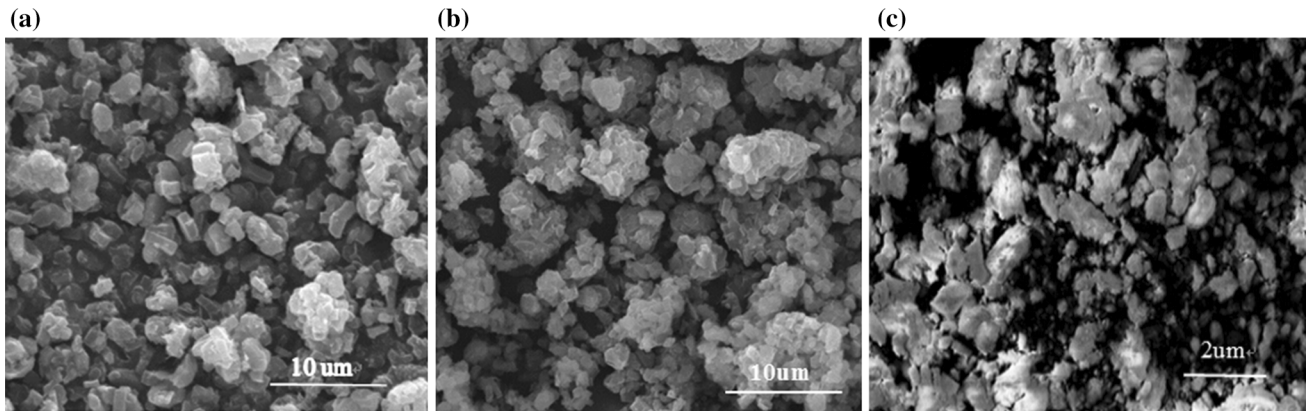

Fig. 4 SEM profiles of the prepared catalysts. **a** Co/ZSM-5, **b** Co/Meso-ZSM-5, **c** Co/SiO_2

which resulted in higher reducibility. This considerably enhanced CO conversion over Co/meso-ZSM-5, compared to Co/ZSM-5 (64.2 vs. 43.5 %, respectively). But it was still lower than that of Co/SiO_2 catalyst due to the presence of unreducible cobalt silicates and/or cobalt aluminate.

The product selectivity of catalysts was also presented in Table 2. A large proportion of microporosity was present on Co/ZSM-5 catalyst, the diffusion rate of reactants and products became slower in the pores, which resulted in the decrease of the probability of re-adsorption of the reaction intermediates such as one-olefins to form higher hydrocarbons. Especially, a certain amount of acid sites made it possible for the acid catalyzed reaction, such as cracking reaction. Moreover, the slow transportation of products

Table 2 The catalytic performance of cobalt catalysts

Catalyst	X_{CO} (%)	Selectivity (%)					O/P[b]	C_{iso}/C_n[c]
		C_1	C_{2-4}	C_{5-18}	C_{18+}	CO_2		
Co/meso-ZSM-5	64.2	10.6	8.9	73.7	6.8	3.4	0.8	0.40
Co/ZSM-5	43.5	15.4	11.2	67.0	6.4	6.8	0.9	0.36
Co/SiO_2[a]	63.2	8.6	4.8	65.9	18.6	2.1	1.2	0.21
Co/SiO_2	92.9	19.3	2.7	67.2	10.8	2.3	1.4	0.24

Reaction conditions: $H_2/CO = 2$, GHSV = 1,000 h^{-1}, T = 210 °C, and P = 2.0 MPa, time-on stream: 24 h

[a] The catalytic data at 190 °C

[b] O/P stands for the olefin-to-paraffin ratio in the range of C_{1-30} hydrocarbons

[c] C_{iso}/C_n stands for isoparaffin to n-paraffin in the range of C_{5-18} hydrocarbons

inside the long micropores of zeolites usually caused over-cracking, leading to high selectivity to undesirable light hydrocarbons. The large amount of mesoporosity created in intraparticles was beneficial to the diffusion of the reactants and products, especially for the bulky molecules, and thereby improved the accessibility to the acid sites and hindered the over-cracking. Thus, the C_{5-18} hydrocarbons were the main compounds over Co/meso-ZSM-5 catalyst (Fig. 6). Both Co/ZSM-5 catalyst and Co/meso-ZSM-5 catalyst showed the lower selectivity to C_{18}^+ fraction.

As for methane selectivity in FT synthesis, many suppositions have been used to explain the formation of methane [7, 20–22]. It was generally assumed that high CH_4 selectivity was mainly attributed to high H_2/CO ratios in reaction system. On one hand, the presence of stable unreduced oxide phases was capable of catalyzing water–gas shift reaction, and thereby increasing the H_2/CO ratio at the catalyst surface. On the other hand, diffusion limitations for carbon monoxide in catalyst pores could also increase H_2/CO ratio in catalyst pore and thus increase methane selectivity. In this study, higher CH_4 selectivity was obtained over Co/ZSM-5 catalyst, which was attributed to its strong cobalt-support interaction resulting in low reducibility and narrow micropores leading to high H_2/CO ratio. However, Co/SiO_2 catalyst also showed much higher selectivity of CH_4 at 210 °C compared to other catalysts due to its concomitant higher CO conversion resulting in releasing large amount of reaction heat. The trend that CH_4 selectivity increased with the syngas conversion was also found by Elbashir et al. [23]. To better understand the difference of their catalytic performance, the product spectrum of Co/SiO_2 catalyst at similar conversion levels was given. The lowest CH_4 selectivity was observed over Co/SiO_2 catalyst due to its highest cobalt reducibility and larger pore size of the support. In contrast to Co/SiO_2 catalyst, Co/meso-ZSM-5 catalyst showed lower C_{18}^+ selectivity and higher CH_4 selectivity due to lower reducibility resulting from irreducible cobalt-support interaction compounds.

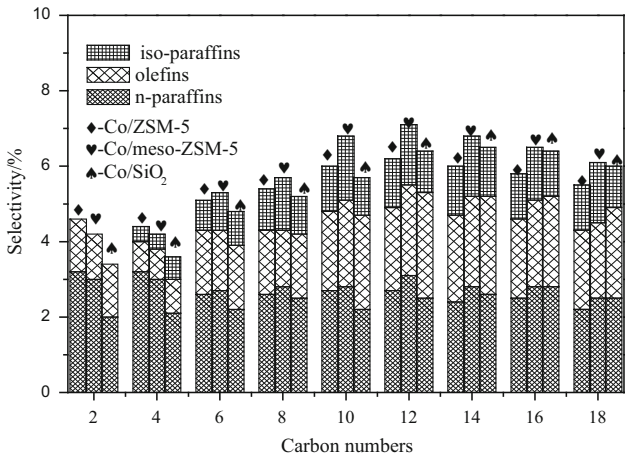

Fig. 6 Carbon selectivity of catalysts in FT synthesis

The selectivity of CO_2 was relatively lower both over Co/SiO_2 catalyst and Co/meso-ZSM-5 catalyst. The easily reducible cobalt crystallites to metallic state at lower temperatures resulted in high reducibility, which was possibly contributed to lower CO_2 selectivity. In the case of Co/ZSM-5 catalyst, higher CO_2 selectivity was observed due to the fact that CO adsorption on the unreduced oxide phase could accelerate the water–gas-shift reaction. The other differences in the catalytic performance of the catalysts involved the ratio of olefins to paraffins (O/P) and the ratio of isoparaffins to n-paraffins (C_{iso}/C_n; see Table 2; Fig. 6). The olefin to paraffin ratio (O/P) of hydrocarbons was the highest over Co/SiO_2 catalyst and decreased over Co/ZSM-5 catalyst and Co/meso-ZSM-5 successively. The lower O/P ratio of Co/ZSM-5 catalyst than that of Co/SiO_2 suggested that zeolite-supported Co catalysts were more active in the hydrogenation reaction. This was mainly attributed to the presence of stable unreduced phases resulting from stronger cobalt-support interaction was capable of catalyzing water–gas shift reaction, and thereby

increasing H_2/CO ratios at the catalyst surface. Moreover, the acid sites on the support played an important role of catalytic cracking reaction of olefinic hydrocarbons to light hydrocarbons. Thus, both strong cobalt-support interaction and acid sites were contributed to the decrease of olefin selectivity. The ratio of isoparaffins to n-paraffins in the range of C_{5-18} (denoted as C_{iso}/C_n), an indicator of the quality of middle distillates, also increased with the increase of acid sites due to the secondary reactions, including hydrocracking and isomerization of the primary hydrocarbons over the acid sites.

4 Conclusions

In this study, the catalytic performance of cobalt catalyst supported on mesopores ZSM-5 in FT synthesis has been studied. Application of such catalyst reduced the wax production compared with that of conventional Co/SiO_2 catalyst. The hierarchical structure combining with the acidity of meso-ZSM-5 improved the selectivity to C_{5-18} fraction, which was ascribed to large mesopores suppressing the hydrocarbon cracking and prevented CH_4 formation. The relative large cobalt crystallites over Co/SiO_2 catalyst and Co/meso-ZSM-5 catalyst resulted in high reducibility, which was possibly contributed to lower CO_2 selectivity. Meanwhile the acid sites of the support played an important role in catalytic cracking reaction of olefinic hydrocarbons to light hydrocarbons. The lowest olefin to paraffin ratio of hydrocarbons was observed over Co/meso-ZSM-5 catalyst.

Acknowledgments The work was supported by the National Natural Science Foundation of China (21106177, 21203232), the Open funds of Key Laboratory of Biofuel (CASKLB201306) and The Basic Research Funds for Central University (2010QNA17), A Project Funded by the Priority Academic Program Development of Jiangsu Higher Education Institutions (PAPD).

References

1. M. E. Dry, G. Ertl, H. Knözinger, F. Schth, J. Weitkamp, *Handbook of Heterogeneous Catalysis*, vol. 6, (Wiley-VCH, Weinheim, 2008), p. 2965
2. R.J. Madon, E. Iglesia, J. Catal. **139**, 576 (1993)
3. Q. Zhang, J. Kang, Y. Wang, Chem. Cat. Chem. **2**, 1030 (2010)
4. A.Y. Khodakov, W. Chu, P. Fongarland, Chem. Rev. **107**, 1692 (2007)
5. B.H. Davis, Fuel Process Technol. **71**, 157 (2001)
6. R. Snel, Catal. Rev. Sci. Eng. **29**, 361 (1984)
7. R.C. Reuel, C.H. Bartholomew, J. Catal. **85**, 78 (1984)
8. L. Gora, B. Sulikowski, E.M. Serwicka, App. Catal. A Gen. **325**, 316 (2007)
9. J. Arandes, I. Torre, M.J. Azkoiti, J. Erena, M. Olazar, J. Bilbao, Energy Fuels **23**, 4215 (2009)
10. A. Corma, J. Martinez-Triguero, C. Martinez, J. Catal. **197**, 151 (2001)
11. G.G. Juttu, R.F. Lobo, Micro. Meso. Mater. **40**(1–3), 9 (2000)
12. P. Arendt, K.H. Van Heek, Fuel **60**, 779 (1981)
13. A. Arenillas, F. Rubiera, J.J. Pis, J. Anal. Appl. Pyrolysis **58**, 685 (2001)
14. G.H. Yang, J.J. He, Y. Yoneyama, Y.S. Tan, Y.Z. Han, N. Tsubaki, Appl. Catal. A Gen. **329**, 99 (2007)
15. S. Kang, J. Ryu, J. Kim, I. Jang, A.R. Kim, G. Han, J. Bae, K. Ha, Energy Fuels **26**, 6061 (2012)
16. J. Kang, K. Cheng, L. Zhang, Q. Zhang, J. Ding, W. Hua, Y. Lou, Q. Zhai, Y. Wang, Angew. Chem. **123**, 5306 (2011)
17. S. Sartipi, K. Parashar, M. Valero Romero, V.P. Santos, B. Linden, M. Makkee, F. Kapteijn, J. Gascon, J. Catal. **305**, 179 (2013)
18. D. Verboekend, S. Mitchell, M. Milina, J.C. Groen, J. Pérez-Ramírez, J. Phys. Chem. C **115**, 14193 (2011)
19. X. Wang, W. Li, G. Zhu, S. Qiu, D. Zhao, B. Zhong, Micro. Meso. Mater. **71**, 87 (2004)
20. A.Y. Khodakov, A. Griboval-Constant, R. Bechara, V.L. Zholobenko, J. Catal. **206**, 230 (2002)
21. R.B. Anderson, W.K. Hall, A. Krieg, B. Seligman, J. Am. Chem. Soc. **71**, 183 (1949)
22. L. Fu, C.H. Bartholomew, J. Catal. **92**, 376 (1985)
23. N.O. Elbashir, P. Dutta, A. Manivannan, M.S. Seehra, C.B. Roberts, Appl. Catal. A Gen. **285**, 169 (2005)